Deciphering shell proteome within different Baltic populations of mytilid mussels illustrates important local variability and potential consequences in the context of changing marine conditions

Jaison Arivalagan, Benjamin Marie, Giovanni Chiappetta, Joëlle Vinh, Xavier Gallet, Matthieu Lebon, Saloua M'Zoudi, Philippe Dubois, Sophie Berland, Arul Marie

Deciphering shell proteome within different Baltic populations of mytilid mussels illustrates important local variability and potential consequences in the context of changing marine conditions.

Jaison Arivalagan[1,2,†], Benjamin Marie[1], Giovanni Chiapetta[3], Joëlle Vinh[3], Xavier Gallet[4], Matthieu Lebon[4], Saloua M'Zoudi[5], Philippe Dubois[5], Sophie Berland[2], Arul Marie[1*]

[1]UMR 7245 CNRS/MNHN Molécules de Communications et Adaptations des Micro-organismes, Sorbonne Universités, Muséum national d'Histoire naturelle, 75005 Paris, France

[2]UMR 7208 CNRS/MNHN/UPMC/IRD Biologie des Organismes Aquatiques et Ecosystèmes, Sorbonne Universités, Muséum national d'Histoire naturelle, 75005 Paris, France

[3]USR3149, ESPCI ParisTech, 75005 Paris, France

[4]UMR 7194, Département de préhistoire, Musée de l'Homme, 75116 Paris, France

[5]Laboratoire de Biologie marine CP160/15, Université Libre de Bruxelles, B-1050 Bruxelles, Belgium

[*]To whom correspondence may be addressed. Email: arul.marie@mnhn.fr

Corresponding author:

Dr. Arul Marie

UMR 7245 MCAM

Plateforme de spectrométrie de masse bio-organique

Muséum National Histoire Naturelle

63, Rue Buffon

75005 Paris, France

Tel: +33140793146

1. Introduction

The mollusc shell, primarily comprising calcium carbonate ($CaCO_3$) and an organic matrix of proteins, carbohydrates etc., exhibits outstanding mechanical properties. Shell formation involves genetically controlled secretion and export of mineral precursors and organic molecules. In bivalves, this process involves the development of an organic framework, comprised of proteins, glycoproteins, lipids, carbohydrates, which act as a template for the nucleation of $CaCO_3$ minerals (Lowenstam, 1981). The different $CaCO_3$ polymorphs and their associated organic compounds are arranged in distinctive patterns, resulting in a vast number of shell microstructures (Carter, 1980). While calcification rate is governed by the calcium carbonate saturation state at the site of shell formation (Morse et al., 2007; Waldbusser et al., 2015), shell organic compounds, typically called shell matrix proteins (SMPs), favour mineral precipitation, even under low calcium carbonate saturation state conditions (Evans, 2017; Thomsen et al., 2017).

In molluscs, SMPs are secreted by the outer mantle epithelial layer and their secretion is both temporal and spatial during the development of the shell (Evans, 2019). Proteins such as silk-fibroin along with beta-chitin polysaccharide forms a gel-like phase and contributes to controlled nucleation (Addadi et al., 2006; Perovic et al., 2014). CaCO3 shell microstructures are classified based on their morphology, and include prismatic, spherulitic, cross-lamellar, homogenous and nacreous forms (McDougall et al., 2018; Chateigner et al., 2000). A large number of SMPs are found to be specific to aragonite such as moderately acidic MSI60, N14, AP7, and basic lustrin A, perlucin, N19, for examples (Marin et al., 2008). Specific protein domains such as VWA, IGF-BP, C-type lectin domains are often found in these SMPs. Similarly, Aspein, prismalin-14, P43 etc., are calcite specific and are enriched in acidic amino acids (extremely acidic) and disposed to bind to metal ions such as calcium. In *M. galloprovincialis,* SMPs such as calponin-like 8, BSMP like, Fibronectin-like, GA-rich etc., were identi-

fied in the nacreous layer and calponin-like-16, chitin synthase-like, Gigasin-like, GFS-rich etc., in the fibrous prismatic layer. Also, calponin–like 6, cathepsin-like-1, Fibronectin-like-1, RKA-rich, etc., were found in both the layers (Gao et al., 2015). One striking feature of molluscan SMPs is the occurrence of repetitive, low complex domains (Jackson et al. 2010) having low amino-acid diversity conferring them strong static conformations or flexible regions lacking well-defined folding structures (Coletta A et al., 2010). The SMPs not only control biomineralization but also confer the shells unique properties such as ductility, or fracture resistance etc.

The Baltic Sea is semi-enclosed and one of the largest brackish water bodies of the planet. Post glacially, the Baltic underwent dramatic changes from marine to fresh and finally to brackish water. This was due to limited water exchanges with the North Sea and also a relatively large fresh water supply (≈15000 $m^3 s^{-1}$) which has resulted in a salinity gradient from high salinity in the west to low salinity in the east with an average salinity of 7.4 psu (Gustafsson & Westman, 2002). As a result of the post-glacial history and brackish water environment, biodiversity and species richness is low compared to the North Sea, yet in terms of biomass, they are comparable (Ojaveer et al., 2010). Low salinity and low total alkalinity (seawater pH buffering capacity) leads to unfavorable conditions for calcifying organisms due to under saturated seawater conditions for calcium carbonate (Tyrrell et al., 2008, Müller et al., 2016; Sanders et al., 2018). Despite suboptimal conditions for calcification and the physiological stress associated with low salinity, marine calcifying *Mytilid* mussels are extensive in many benthic ecosystems and are key organisms for nutrient recycling and supporting biodiversity (Vuorinen et al., 2002, Norling & Kautsky, 2008). Baltic Sea forms a hybrid zone between *Mytilus edulis* and *Mytilus trossulus* (Väinölä & Strelkov, 2011) with *M. edulis* allele frequencies being higher at high salinity and *M. trossulus* allele frequencies being higher at low salinities in the Central and Eastern Baltic (Stuckas et al., 2009). Gene introgression is so

extensive between both species that pure individuals of either species are not present at all and genetic divergence from neighboring North Sea populations is high (Johannesson & André, 2006, Stuckas et al., 2017). This noticeable genetic divergence suggests local adaptation of Baltic *Mytilid* (referred as Baltic mussels) populations to low salinity and recent findings suggest that Baltic populations from low salinity (7 psu) are more tolerant of low seawater [Ca^{2+}] (characteristics of extremely low salinities) compared to populations from higher salinity (16 psu) (Thomsen et al., 2017). Baltic blue mussels calcify slowly and attain a size which is one third that of North Sea mussels with thin and elongate shells (Kautsky, 1982).

In fact, Baltic blue mussels grow to larger sizes when transplanted to marine waters, emphasizing that calcification rates and maximum shell size are independent from genetic make-up (Kautsky, Johannesson & Tedengren, 1990). One of the most prominent features of the Baltic is, the number of mussel predators such as the starfish *Asterias rubens* and the crab *Carcinus maenas* are comparatively absent in the eastern parts of Baltic where the salinity is less than 10 psu. This lack of predation pressure may have additionally led to a reduction in morphological defenses such as weak adductor muscles and thinner shells (Reimer & Harms-Ringdahl, 2001).

To understand how Baltic blue mussels can form shells under the extremely low calcium carbonate saturation states, it is crucial to deduce the molecular mechanisms underpinning shell formation, especially the fate of SMPs, which are key regulators of the biomineralization process. Many studies under controlled conditions have shown that variations in pH, temperature and salinity affect the shell formation process, growth, survival etc., in bivalves (Mackenzie et al., 2014). In fact, these factors predominately alter metabolic processes and energy partitioning to growth and calcification (Sanders et al., 2018). However, valuable clues offered by the SMPs to understand the molecular mechanisms of adaptation of the calcifiers in the context of changing marine conditions have not received any attention yet. In this work, we investigated

the modulation of the SMPs and how it alters the physical and biochemical properties of the shells in Baltic blue mussels living in brackish water with respect to mussels inhabiting fully marine North Sea.

2. Materials and methods:

2.1. Sample collection

Information about sample collection is described in detail in a recent publication (Telesca *et al.*, 2019). Briefly, Sub-tidal populations of adult Baltic Mytilus spp. (shell length: 30-40 mm, age: 2-4 years) were collected in July-August 2015 from Sylt (German North Sea coast: 54°54′ N 8°20′ E), Usedom (German Baltic Sea coast: 53°56′ N 14°05′ E) and Nynäshamn (Swedish east coast: 53°56′ N 14°05′ E) (Figure 1a). Salinity is relatively stable in the central Baltic Sea and not significantly different between the 2 sites (approximately 5.3 and 5.9 psu for Usedom and Nynäshamn, respectively) but relatively very low compared to North Sea site (Sylt, salinity is approximately 29.3 psu). Based on water samples and measurements taken at the time of sampling, pH and temperature were not largely different (although both parameters are much more variable at both Baltic sites compared to the North Sea site, Sylt) between Baltic sites. Carbonate chemistry (pH, CO_2 and calcium carbonate saturation state) is more stable in the North Sea due to the higher total alkalinity and a higher buffering capacity to pH change. Age determination was an estimate based on growth rates for each population and shell lengths of samples (See Vuorinen et al. 2002). Shell length was kept constant between sampled populations to enable direct comparison. Soft tissue was removed immediately from the shells using a scalpel and shells were air dried at room temperature for a minimum of 2 weeks before analysis.

2.2. Shell mechanical tests

The fracture force of the left valve of the specimens (n=6) from each location was tested using a simple compression method. All shell valves were placed on a steel block on the stage of the force stand (Instron 5543) in an identical orientation (shell length along the horizontal axis, outer shell surface facing upwards). Mechanical tests were carried out using a second metal block, fixed on the load frame of the force stand, which was lowered onto the valve at a speed of 0.3 mm min^{-1} (simple compression test) until fracture occurred. Displacement and force were recorded continuously using a 100N load cell at a frequency of 10 Hz.

2.3. FTIR analysis for mineral composition

0.5 mg of the shell powder for each location (n=5) was analyzed using an ATR-FTIR Vertex 70 spectrometer (Bruker). The samples were measured using a Single Reflection diamond ATR system (Golden Gate, Specac). Each spectrum comprised 64 scans at 4 cm^{-1} resolutions. The peak values such as 711 cm^{-1}, 700 cm^{-1}, 856-875 cm^{-1}, 1401-1754 cm^{-1}, 1785-1793 cm^{-1} were used to distinguish between calcite and aragonite polymorphs. Loftus and coworkers have demonstrated a method to establish calcite and aragonite ratio in shell samples using specific FTIR ATR absorbance peak height ratio (Loftus *et al.*, 2015). We used 875/1785 cm^{-1} (C-O ν2 - out-of plane- bending in calcite / combination of stretching vibrations ν1 and ν4 in aragonite respectively) and 1793/1785 cm^{-1} (combined ν1 and ν4 stretching vibrations in calcite *vs* aragonite) peak ratios to consistently provide validated estimates of a similar mix of the two polymorphs in the samples.

2.4. Scanning electron microscopy

Three mussel shells with same shell size from each location were mechanically fragmented. Prior to analysis, the freshly fractured transections were gold-coated. Scanning electron microscopy was carried out using a Hitachi SU3500 (Hitachi, France). In order to avoid parallax error resulting from irregular fractured surface, the angle of the electron beams was tilted ac-

cordingly. The periostracum and shell thickness measurements were performed in the area where the thickness of nacre and prism were 1:1 ratio. This was used to frame a "region of interest" and five measurements were made at different positions spread over each frame (region of interest) for each individual (total measurement for each site =15).

2.5. Sample preparation for total organic content and proteomics:

Five individual shells collected from each location were washed separately with 5-10% sodium hypochlorite (NaOCl) to remove surface organic impurities and periostraca. Shells were then washed with milli-Q® water and air-dried. The shells were then cut into small pieces and polished with a dremel drill. Before pulverizing the shells to a powder, they were washed briefly with NaOCl and milli-Q® water and air-dried. Powdered shell fragments were graded using 250-µm mesh. 400 mg of shell powder was decalcified using 5% cold acetic acid (5 ml) for an hour and 10% cold acetic acid (5 ml) overnight to ensure complete dissolution of $CaCO_3$. The homogenate was centrifuged (14,000 rpm, 20 mins, 4°C) to separate the acid soluble (ASM) supernatant and the acid insoluble matrix (AIM) pellet. The AIM was washed with milli-Q® water several times to remove all traces of the acid and freeze-dried. The ASM was washed with milli-Q® water on a 10 kDa filter (Sartorius, VIVASPIN 20) to remove the acid and freeze-dried. The dry samples (ASM and AIM) were weighed to estimate the total organic content.

For proteomics, both dried AIM and ASM were denatured using 30 µL of 8 M urea and then 15 mM dithiothreitol (DTT) in 100 mM triethyl ammonium bicarbonate (TEAB), both the steps were carried out at 37°C for 1h each. Alkylation was done using 20µL of 15 mM iodoacetamide in the dark and at room temperature for 1h. The resulting solution was diluted with 100 mM ammonium bicarbonate to reduce the concentration of urea to 2M and digestion was carried out by adding 10 µg of trypsin (Sigma-Aldrich, France) to the AIM and ASM samples and incubated at 37°C overnight. The resulting digested peptides were acidified with 10 µL of

10% formic acid and desalted using 4mm Empore™ SPE (Sigma-Aldrich, France) cartridges. Desalted peptides from both ASM and AIM fractions from each sample were mixed into a single sample and quantified using a Bicinchoninic acid kit (Sigma-Aldrich, France) to determine total protein content.

For mass spectrometry analysis, peptides were concentrated on a C_{18} cartridge (Acclaim PepMap100, 5µm particles, 300µm i.d. x 5 mm, Thermo Scientific) at 15 µl/min flow rate in, 0.05% aq. TFA: ACN (98:2, v/v) (buffer A) for 5 minutes followed by elution to a C_{18} column (Acclaim PepMap100, C_{18}, 3 µm particles, 75 µm i.d. x 50 cm length, ThermoFisher Scientific) at a flow rate of 220 $nL.min^{-1}$. Peptides were then separated using buffer B (ACN/0.1% and aq. FA (90:10 v/v)) with the following gradient: 2-40% buffer B for 170 min, then 40-50% buffer B for 10min. The eluted peptides were analyzed by a nano-ESI quadrupole-Orbitrap mass spectrometer (Q Exactive, Thermo Fisher Scientific) with the following parameters: one full MS acquisition (Resolution 70,000 at m/z 200, Automatic gain control target value 1e6, max. injection time 250 ms), followed by 10 MS/MS (TOP 10, CID) with isolation window 2 m/z, fixed first mass 100 m/z, resolution 17,500 at m/z 200, AGC target value 5.10^4 counts, maximum injection time 120 ms, CE 30 and dynamic exclusion of 60 s.

2.6. Proteomic data analysis

The MS/MS spectra obtained from the five individual samples from the three locations were searched against a mantle transcriptome database of *M. edulis* and *M. trossulus* published recently (Knöbel, L et al., 2020) using an in-house Mascot server (Matrix Science, London, UK; version 2.4.1). The database search was carried out using following parameters: missed cleavage = 1, carbamido-methylation of cysteine as fixed modification and oxidation of methionine, de-amidation of aspartic acid and asparagine as variable modifications, mass tolerance of MS and MS/MS experiments as 20 ppm and 0.5 Da. Scaffold software (Proteome Software Inc., Portland, USA; version 3.6.5) was used to validate and group the matched pro-

teins. The following criteria were set for each sequence scaffold for validating the proteins: peptide identification probability greater than 95% as specified by Peptide Prophet algorithm and protein identification probability greater than 95% as specified by Protein Prophet algorithm with minimum two unique peptides (containing at least eight amino acids) matched. BLAST2GO tool (Omicsbox, Bio Bam, Valencia, Spain; version 4.0.7) was used to carry out sequence similarity protein searches against NCBI protein database. In addition to in-built InterPro results from BLAST2GO, Conserved Domain Database searches (https://www.ncbi.nlm.nih.gov/Structure/cdd/cdd.shtml) were performed to predict the conserved protein domains in the target protein sequences.

A label free semi-quantitative approach was performed in PEAKS studio software (Bioinformatics Solutions Inc., Waterloo, Canada; version 7) to identify differentially expressed proteins. The differential expression protein patterns were based on log2 ratio to average signal intensity area across samples. The results were validated using the following parameters: [1] The peptide significance threshold $\geq$ 10×10logP and protein significant threshold $\geq$ 20×10logP. [2] The MS signal filter was set to $\geq 10^6$ average intensity area and $\geq$ 0.5 quality of the signal. [3] Mass error tolerance is 20 ppm. [4] Confident sample number $\geq$ 3. [5] Protein fold change $\geq$ 2. Normalization was done using TIC. FDR threshold is 1%. The reference sample for relative quantification was auto-detected by the software based on the sample profile.

2.7. Statistical analysis

Differences in the gross shell features from different locations related to fracture force, FTIR and shell traits were analyzed using Kruskal-Wallis non-parametric rank test to determine whether there were significant differences among the shells from different locations. This test was chosen as the need for the data to follow normal distribution is not required but the assumption of independent observations was met. Null hypothesis of equal mean ranks was

considered and the low *p*-value allowed to reject the null hypothesis. PCA analysis was performed as multivariate analysis to fit shell traits (thickness and organic content) covariance matrix into orthogonal decomposition according independent loadings for further exploratory data analysis.

Statistical tests were carried out using R v3.6.0 (R: A language and environment for statistical computing. R Foundation for Statistical Computing, Vienna, Austria. URL https://www.R-project.org/] using the *Kruskal.test()* from the native package 'stats'. The graphical results were generated using the package 'lattice'.

3. Results :

3.1. Shell mechanical test

Shell fracture tests waere carried out to find if significant differences exist between the three populations, reflecting shell resistance. Differences in shell length (n=7) were not observed to be significantly different among the three sites (Fig.1b, Kruskal-Wallis chi-squared= 0.28, p=0.86) excluding it as contributing to shell fracture results. Breaking load (F_{max}) indicated that Baltic blue mussels (Nynäshamn and Usedom) exhibit lower shell-fracture resistance than North Sea (Sylt) mussels (Kruskal-Wallis chi-squared =8.43, p = 0.01, Supplementary Data 1).

3.2. Mineral composition

Crassostrea gigas (calcite) and *Mya truncata* (aragonite) shell powders were used as a reference in FTIR-ATR analysis to measure the absorbance peak profiles of calcite and aragonite $CaCO_3$ polymorphs in *Mytilus* shells (Figure 1c, d). The absorbance peaks measured from the Baltic and North Sea mussel shells were identical to both calcite and aragonite profiles of the reference species, confirming the presence of both polymorphs. Significant variation in cal-

cite/aragonite ratio of the shells from different sites could potentially contribute to difference in shell mechanical properties. However, absorbance ratios for 875/1785 cm^{-1} showed no difference in the calcite/aragonite ratio (Kruskal-Wallis chi-squared = 0.78, p= 0.67) with respect to different locations (Figure 1e, f). Similar results were obtained for absorption ratio 1793/1785 cm^{-1} (kruskal-wallis chi-squared = 0.86, p= 0.65, Figure 1e, f).

3.3. Shell traits (periostracum, shell thickness, organic content and microstructure)

Shell morphometric patterns of n=3 equally sized animals collected from North Sea and Baltic Sea were analyzed. For each shell, data from five different points on the shells were collected. Shell thickness varied significantly among the three sites (Kruskal-Wallis chi-squared = 35.27, p= $2.19e^{-8}$) and periostracum thickness also showed the same trend (kruskal-wallis chi-squared = 30.42, p= $2.47e^{-7}$; supplementary Data 2). Plotting periostracum/shell thickness ratio (as %) separates the shells according to their location (supplementary figure 1a) and same trend is observed by plotting mineral content of the shells.

The organic content obtained after decalcification of the shells (periostracum being removed during shell cleaning process) varied significantly among the three sites (Kruskal-Wallis chi-squared = 5.06, p= 0.07, supplementary Data 3). Higher organic contents were found in Nynäshamn shells followed by Usedom and Sylt shells (Supplementary Figure 1b). It can be seen that the shell traits from different locations vary significantly as a principal component analysis of these traits clearly revealed clustering of the mussels into three different groups (supplementary Figure 1c). The first component gets a clear opposition in scores projection between Sylt mussel shells on one part Nynäshamn and Usedom mussel shells on the other part explained by a contrast between the mineralized layer thickness and the organic content. The second component gets a clear opposition in scores projection between Usedom mussel

shells on one part and Nynäshamn and Sylt mussel shells on the other part, which is mainly explained by the variable 'periostracum thickness'.

Scanning electron microscopy images of Baltic blue mussel shells indicates altered in the microstructure as evidenced by relatively thin aragonite tablets and irregular calcite prisms compared to shells of North Sea mussels (Figure 2).

3.4. Shell matrix proteins

To identify the shell matrix proteins presents in the shells of *Mytilid* mussels from Baltic Sea and North Sea, we interrogate the transcritpome databases of both *M. edulis* and *M. trossulus* against the shell proteomics dataset. The number of transcripts matched with at least two unique peptides for each site using *M. edulis* database are: 247 (Sylt), 436 (Usedom) and 187 (Nynäshamn); transcripts matched using *M. trossulus* database are: 188 (Sylt), 224 (Usedom) and 257 (Nynäshamn). In total, 671 and 624 transcripts with at least 2 unique peptides could match using *M. Trossulus* (FDR peptide > 0.2%, protein =0.1%) and *M.edulis* (FDR peptide >0.4%, protein = 0%) databases, respectively (Supplementary Table 1). It should be noted that the matched transcripts include both proteins and proteoforms. The difference in the number of transcripts matched with respect to different sites and databases could be partially attributed to the taxonomy specificity of the mussels inhabiting the three sites: Sylt is populated by *M. edulis*, Nynäshamn by *M. trossulus* and Usedom by *M. edulis* x *M. trossulus* hybrid complex (Telesca et al., 2019). Carrying out BLAST using the matched sequences resulted in the annotation of 327 and 462 sequences for *M. trossulus* and *M. edulis*, respectively (Supplementary Table 2). Among the annotated sequences, 144 SMPs are common to the shells from the three sites with *M. edulis* database and 131 SMPs in case of *M.trossulus*. Gene ontology count assigned top five molecular functions such as oxidoreductase activity, metal ion binding, chitin binding, peptidase activity and catalytic activity for transcripts matching *M. edulis* database (total sequence count = 58) and in case of *M.trossulus* database the molec-

ular functions were similar excepting that mono phenol monooxygenase activity replaced catalytic activity (total sequence count =74, Figure 3).

Label free semi-quantitative analysis of shell proteins from the three sites showed differential expression of many SMPs that could be attributed to different functional categories. 37 SMPs were found to be modulated when annotated against *M. trossulus* transcriptome database including SMPs comprising HHIP-like protein, shell protein-4, GA-rich protein, protease inhibitor-like protein B1, matrix protein-1, metalloprotease inhibitor-3-like protein in addition to a WAP domain containing protein (Figure 4, Supplementary Table 3). 17 SMPs were modulated when annotated using *M. edulis* transcriptome, and interestingly many are subset of the modulated SMPs identified in *M. trossulus* (Supplementary Figure 2, Supplementary Table 1).

4. Discussion:

The salinity gradient in the different regions of Baltic Sea is well established (Müller et al., 2016) and the adaptation of species to the brackish conditions in the Baltic Sea has caused both morphological and genetic differences compared to salt/water ancestors (Larsson et al., 2017). Under unfavorable environment, marine calcifiers reallocate the energy required for different cellular functions and generally this affects shell formation leading to shell phenotypes (Harper et al., 2012). Even though the SMPs employed in shell building by marine calcifiers are species specific, critical steps such as mineral deposition, crystal growth and orientation etc., could be effected by divergent sets of SMPs resulting in altered shell traits. The quantity of SMPs in the shell from natural populations may reflect the global phenotype of the organism during its entire life span and not a particular temporal scale.

Generally, *Mytilus* acclimation to varying temperatures and pH has shown limitation in protein metabolism, thinner shells and $CaCO_3$ crystal disorientation, which may affect the mate-

rial properties of the shell (Fitzer et al., 2015, 2018; Fitzer et al., 2014a). Noticeably, our data revealed significant differences in shell morphology, microstructures and protein content in Baltic blue mussels from different population experiencing different salinity conditions. The production of a calcium carbonate exoskeleton depends not only on the seawater carbonate chemistry but also on the ability to produce bio-minerals (Fitzer et al., 2014b), and might be directly related to SMP content of individual shells.

4.1. Quantification of SMPs and shell phenotype

Quantitative protein expression profiling is useful to gain insight on molecular mechanisms in marine shell forming organisms. For example, this approach was employed to investigate the impact of reduced seawater pH along with pathogen challenge in the immune response of *Crassostrea gigas* (Cao et al., 2018). In fact, the amount and nature of the SMPs in the shell alter its physical property affecting the resilience of mussels to rapidly changing environmental conditions.

Shell formation involves the production of an extracellular organic matrix (the shell scaffold). This primarily contains β-chitin and SMPs and the crystals are induced to form inside these matrix voids (Falini et al., 1996). Chitinase-3 plays a key role in the metabolism of chitin in the shell scaffold, which provides the template for mineral nucleation. However, its expression may vary in response to different abiotic factors as evidenced by the substantial increase in its expression in the outer mantle epithelial cells of *Pinctada fucata* during shell regeneration experiments (Li et al., 2017) and also during shell remodeling in the freshwater snail *Lymnaea stagnalis* (Yonezawa et al., 2016). In contrast, under pH stress the chitinase-3 gene expression was found to be down regulated in mussels (Hüning et al., 2013). In Baltic blue mussels, chitinase-3 was found in relatively higher amounts in the shell indicating altered scaffolding processes contributing to the shell phenotype in low salinity.

Label free quantification of the protein extracts from the shells collected from the North Sea (Sylt) and Baltic Sea (Usedom and Nynäshamn) indicated modulation in many SMPs (discussed below). At this juncture, it is pertinent to examine if any disparity in aragonite or calcite content in the shells could affect the quantity of certain polymorph-specific SMPs. The FTIR data indicated that aragonite/calcite ratios did not vary significantly in the shells of individuals from the three different locations and thus, it can be inferred that the relative modulation of SMPs could basically not be influenced by a specific calcium carbonate polymorph. Shell matrix proteins such as blue mussel shell protein (BMSP), sushi-like protein and chitinase-3 or several Von Willebrand factor-A (VWA) and chitin binding domain-2 (Chbt-2) containing proteins showed remarkable distinct quantity in the shells of individuals collected from the three sampling locations (Figure 4, Supplementary Figure 2 and Supplementary Table 3). In fact, proteins containing domains such as VWA and Chbt-2 contribute to the silk-like protein complexes (Weiner, 1979) and may act as glue assembling β-chitin sheets and minerals (Suzuki et al., 2011); their relatively higher content in Baltic blue mussels suggests that the scaffolding of β-chitin within the shell matrix space may be distinguishable too. Hydrophobic glycine-alanine rich (GA-rich) proteins sandwich β-chitin and support the β-sheet conformation, whereas, serine-aspartic acid rich (SD-rich) proteins are believed to surround the above complex and interact with the mineral phase aiding in crystal formation (Falini et al., 1996; Nakahara et al., 1980; Weiner, 1979; Weiner & Traub, 1980). Intriguingly, these two chitin interacting proteins showed relatively lower contents in the Baltic blue mussels leading potentially to altered microstructural organization in the shell as observed on the scanning electron microscopy images (qualitative observations; Figure 2). Information about the orientation of $CaCO_3$ crystals from these shells would better explain the altered microstructures.

343 The thicker periostracum found in Baltic blue mussels are almost certainly associated with the
344 increased protection compensating when the calcium carbonate saturation state is low (Thom-
345 sen et al., 2010) and shell dissolution is more likely. Interestingly, tyrosinase and byssal pe-
346 roxidase-like proteins levels were higher in Baltic mussel shells (Figure 4, Supplementary
347 Table 3). This suggests that the processes important for periostracum maturation i.e. oxidation
348 of tyrosine to L-Dopa and L-Dopa to O-quinone (Qin et al., 2016; Zhang et al., 2006) are also
349 valuable for shell matrix formation, particularly under the low calcium carbonate saturation
350 states encountered in the Baltic Sea. Tyrosinases have also been extracted from the shells of
351 other *Mytilus* species (Gao et al., 2015) and acclimation of Baltic blue mussels to low pH
352 (which produces a dramatic reduction in calcium carbonate saturation state) resulted in a very
353 strong (>100 fold) increase in the mRNA expression of a mantle tissue-specific tyrosinase
354 isoform (Hüning et al., 2013). Generally, a higher (shell) organic content, together with re-
355 duced calcium and inorganic carbon availability lead to increased energy demands and this
356 may explain the dwarfism in *Mytilus spp.* in the low saline Baltic Sea (Kautsky et al., 1990).
357 Considering the projected decrease in salinity along with increased physiological osmotic
358 stress, *Mytilus spp*. inhabiting the Baltic Sea are more likely to form a thicker periostracum
359 (Telesca et al., 2019) pointing out that further adaptation by *Mytilus spp*. with regard to shell
360 biomineralization should be anticipated.

361 Surprisingly, several other key-domain shell proteins were not observed to present quantifica-
362 tion difference between the different location populations, including carbonic anhydrase
363 (CA), epidermal growth factor (EGF) and fibronectin-3 (FN3). While CA converts carbon
364 dioxide to bicarbonate ions (Miyamoto et al., 1996), EGF may interact with calcium ions, and
365 fibronectin brings anions and cations into close proximity to enhance nucleation as proposed
366 for calcium phosphate biomineralization (Ba et al., 2010). Due to this apparently ubiquity of
367 the observed quantity in shell of CA, it may be presumed that bicarbonate ion nucleation

might not be a decisive factor for processes underlying shell phenotypic plasticity under low salinity conditions. Alternatively, it is also possible that the shell protein composition does not reflect the actual quantity of different isoforms of CA in the mantle tissue. Even though the *M. edulis* shell is composed of both calcite and aragonite layers, calcite-specific EGF containing protein was not differentially quantified within the shell of the sampled populations.

Although to date, the complete set of proteins within the mollusc shell biomineralization tool kit remains to be described in-depth, recent studies have demonstrated the presence of an evolutionarily conserved toolkit for shell formation that is crystal-specific and species-specific from four highly divergent bivalves including *M.* edulis (Arivalagan et al., 2017). In addition, Feng *et al.,* observed that proteins containing domains such as carbonic anhydrase, sushi, VWA and chitin binding domains are conserved in the shell matrix of many bivalve species (Feng et al., 2017). In this study, proteins such as BMSP, sushi-like protein, chitinase-3 and tyrosinase, which contain domains that are potentially part of the basic tool kit present quantity variations within the shell of the three different Baltic populations sampled, suggesting that variation in the overall biomineralization processes between those populations, supporting the shell structure and morphology differences observed in parallel.

4.2. Shell fracture resistance

The mechanical properties of bivalve shells are also attributed to the minor organic components present in the $CaCO_3$ inorganic structure that is characterized by highly ordered crystal state. Deviations from this state are considered to indicate impaired or irregular biomineralization resulting in weaker shells (Fitzer et al., 2016). Common structural proteins such as elastin, collagen, silk and keratins are characterized by a long range ordered molecular secondary structures (e.g. β-pleated sheets, β-spirals, coiled coils, triple helices etc.) that accommodate a broader spectrum of functional requirements such as elasticity to support diverse tissues (Hu *et al.*, 2012). The sequence/motif repeats are responsible for the conformation of

their secondary structures. For example, a recent study on teeth-like structural proteins present inside squid suckers using proteomics and molecular biology clearly highlighted the relationship between the molecular features of the low-complexity and repeated proteinaceous sequences and mechanical properties of the resulting biomineral (Jung et al., 2016). The tandem repeats of proteins that are embedded within the squid ring teeth are responsible for the extraordinary toughness and flexibility of the teeth biomaterial. Based on the observed differences in the mechanical properties of the *Mytilus* shells of blue mussels originating from the compared Baltic area (Figure 1b), we hypothesized that the shells, especially those presenting higher mechanical properties might harbor certain enrichment in such structural proteins with a similar set of repetitive sequences and secondary structures. The primary sequences of two proteins (TR78416_c1_g1_i2 and TR71052_c0_g1_i1, Figure 6a and b) that are highly expressed in North Sea mussel shells (homologous to MSI-60 of *P. fucata* and insoluble proteins of *Mytilus spp*) contain several repeat sequences of this kind. The poly-Ala regions in these proteins are similar to that of silk protein, which forms β-sheet structures by placing successive alanine residues on alternate sides of a backbone (Hayashi et al., 1999) with each alanine chain interlocking with an adjacent chain *via* hydrophobic interactions. Similarly, GGXGG repeats, as those found in mussel shell proteins, were previously reported in the insect glycine rich cuticle protein family (CPG) including resilin (a rubber-like protein in insect cuticle), which provides higher elasticity and acts as an efficient elastic-energy storage component in insect wings (Adams, 2000; Andersen and Weis-Fogh, 1964). 3-D model simulations of the protein sequences (TR78416_c1_g1_i2 and TR71052_c0_g1_i1) predicted β-strands in both the cases (Figure 5a and b) and the tertiary structure of TR78416 resembled a β-solenoid, in particular the β-roll structure of spider silk protein (Figure 5c), which confers unique mechanical properties to silk. Disordered regions rich in Asp, Ser and Gly that have the potential to bind $CaCO_3$ minerals, or to allow calcium ion super-saturation conditions

were also found in different amount in the shell of the mussel populations. The capacity of these proteins to bind $CaCO_3$ minerals may play a critical role in making shell more resistant to fracture as observed for Sylt shells. The observation that these proteins were present in relatively lower amounts along with thinner shell in Baltic blue mussels may explain the fragility of those biomineral structures (Figure1b). Variations in shell thickness indicate alteration in biomineralisation control by the SMPs and may alter the fracture force.

4.3. Alteration in biochemical defense

The identification in the mussel matrix of many proteins that could be rely to immune classes raises the question of "what other functions could bear certain SMPs that would not basically be involved in shell building process?" The presence of proteins with immunity-related functions argues for the occurrence of an efficient biochemical defense system operating in the shell, in addition to the primary shell edification processes. Recent studies on gastropods suggest that the shell has been co-opted as a defense system to encase and kill parasitic nematodes which validates the data here (Rae, 2017).

An innate immune cascade involving phenoloxidase (PO) leads to several responses such as pigmentation (melanization) and repair of damaged insect exoskeletons including hardening (sclerotization), pathogen elimination by phagocytes (opsonization) etc., (Cerenius & Söderhäll, 2004; Jiravanichpaisal et al., 2006). POs are a copper containing class of enzymes including tyrosinase, catecholase and laccase (Luna-Acosta et al., 2011). In mussels, tyrosinase is involved in periostracum formation (Zhang et al., 2006) and the presence of laccase-4 like protein (pro-PO) and several other components of the PO cascade imply the participation of certain POs in the mussel immune response. Generally, PO activation starts with the aggregation of several proteins and enzymes, which convert pro-PO to PO (Figure 6), thanks to the action of proteinases. Here, no shell proteinase present observable differences in quantity within either North Sea or Baltic blue mussels. However, serine protease inhibitors containing

443 domains such as kunitz, serpin and TIMP (tissue inhibitor of metalloproteinase), that are neg-
444 ative regulators of the PO pathway (Jiravanichpaisal et al., 2006), were present in high
445 amount in Baltic mussel shells even though pro-PO (Laccase-4 like protein) did not present
446 different quantification within the three populations. It is worth to note that cellular cost of
447 investing energy in systems such as PO is expensive. Generally, organisms opt for constitu-
448 tive defenses and therefore activate the PO cascade only when there is a constant pathogen
449 threat in their environment (Moret, 2003). Baltic waters may contain relatively fewer mussel
450 pathogens and shell boring organisms than the North Sea, which might explain the observed
451 differential regulation of the PO cascade.

452 **5. Conclusion:**

453 To refine predictions of the effects of environmental change on marine calcifiers, it is essen-
454 tial to decipher the intricate relationship between shell phenotype, biological control of bio-
455 mineralization and the environment. This study is the first to show that modulation in SMPs
456 correlates to the shell phenotype and might support environmental adaptability of the mussels.
457 Clearly, our findings show that alteration in the mechanical properties and along with poten-
458 tial biochemical defense offered by the shell are correlated with specific SMP features of the
459 populations. Although Baltic blue mussels have in first order successfully experiment life
460 under low-salinity conditions, they may also have encountered a lower predator environment
461 pressure over several generations, that also may have influenced the composition of the shell
462 calcifying matrices, through selective or adaptative mechanisms. Further declines in salinity
463 over short time-spans in the Baltic Sea (Gräwe et al., 2013) might irreversibly alter the calci-
464 fication processes because of increased energy costs, altered protein metabolism, decreased
465 shell thickness etc. Also, a recent study showed that low salinity induced strong immunosup-
466 pressive effects on the functional and immune molecular traits of *M. edulis* (Wu et al., 2020)
467 endangering further the survival of populations.

To conclude, SMPs seem to constitute valuable indicators of altered molecular mechanisms of shell edification for Baltic blue mussels encountering contrasted marine conditions. Shell traits such as periostracum thickness, organic content, microstructure and fracture resistance qualitatively correlates with the modulation of SMPs. Large scale studies in this context and assessing genetic background will help to discern alteration in biomineralization control by environmental and genetic factors and further enable to identify molecular signatures of resilience or sensitivity in marine calcifiers.

References:

Adams, M.D., 2000. The Genome Sequence of Drosophila melanogaster. Science, 287, 2185–2195. https://doi.org/10.1126/science.287.5461.2185

Addadi, L., Joester D., Nudelman F., Weiner S., 2006. Mollusk shell formation: a source of new concepts for understanding biomineralization processes. Chemistry. 12(4):980-7. doi: 10.1002/chem.200500980.

Andersen, S.O., Weis-Fogh, T., 1964. Resilin. A Rubberlike Protein in Arthropod Cuticle. Adv. In Insect Phys. 2, 1–65. https://doi.org/10.1016/S0065-2806(08)60071-5

Arivalagan, J., Yarra, T., Marie, B., Sleight, V.A.V.A., Duvernois-Berthet, E., Clark, M.S.M.S., Marie, A., Berland, S., 2017. Insights from the shell proteome: Biomineralization to adaptation. Mol. Biol. Evol. 34, 66–77. https://doi.org/10.1093/molbev/msw219

Ba, X., Rafailovich, M., Meng, Y., Pernodet, N., Wirick, S., Füredi-Milhofer, H., Qin, Y.X., DiMasi, E., 2010. Complementary effects of multi-protein components on biomineralization in vitro. J. Struct. Biol. 170, 83–92. https://doi.org/10.1016/j.jsb.2009.12.018

Cao, R., Wang, Q., Yang, D., Liu, Y., Ran, W., Qu, Y., Wu, H., Cong, M., Li, F., Ji, C., Zhao, J., 2018. CO2-induced ocean acidification impairs the immune function of the Pacific

491 oyster against Vibrio splendidus challenge: An integrated study from a cellular and pro-
492 teomic perspective. Sci. Total Environ. https://doi.org/10.1016/j.scitotenv.2018.01.056

493 Carter, J.G., 1980. Guide to bivalve shell microstructures. Skelet. growth Aquat. Org. Plenum
494 Press. New York 142.

495 Chateigner D., Hedegaard C., Wenk H., 2000. Mollusc shell microstructures and crystallo-
496 graphic textures. J Struct Geol, 22:1723-1735

497 Cerenius, L., Söderhäll, K., 2004. The prophenoloxidase-activating system in invertebrates.
498 Immunol. Rev. 198, 116–26.

499 Coletta A., Pinney J.W., Solís D.Y., Marsh J., Pettifer S.R., Attwood T.K., 2010. Low-
500 complexity regions within protein sequences have position-dependent roles. BMC Syst
501 Biol. Apr 13;4:43. doi: 10.1186/1752-0509-4-43.

502 Evans J.S., 2019. The Biomineralization Proteome: Protein Complexity for a Complex Bioc-
503 eramic Assembly Process. Proteomics.;19(16): e1900036. doi:10.1002/pmic.201900036

504 Evans, J.S., 2017. Polymorphs, Proteins, and Nucleation Theory: A Critical Analysis. Miner-
505 als, 7, 62. https://doi.org/10.3390/min7040062

506 Falini, G., Albeck, S., Weiner, S., Addadi, L., 1996. Control of Aragonite or Calcite Poly-
507 morphism by Mollusk Shell Macromolecules. Science 271 (5245), 67-69.
508 https://doi.org/10.1126/science.271.5245.67

509 Feng, D., Li, Q., Yu, H., Kong, L., Du, S., M.Degnan, B., 2017. Identification of conserved
510 proteins from diverse shell matrix proteome in Crassostrea gigas: characterization of ge-
511 netic bases regulating shell formation. Sci. Rep. 7, 45754.
512 https://doi.org/10.1038/srep45754

513 Fitzer, S.C., Chung, P., Maccherozzi, F., Dhesi, S.S., Kamenos, N.A., Phoenix, V.R., Cusack,

514 M., 2016. Biomineral shell formation under ocean acidification: a shift from order to
515 chaos. Sci. Rep. 6, 21076. https://doi.org/10.1038/srep21076

516 Fitzer, S.C., Cusack, M., Phoenix, V.R., Kamenos, N.A., 2014a. Ocean acidification reduces
517 the crystallographic control in juvenile mussel shells. J. Struct. Biol. 188, 39–45.
518 https://doi.org/10.1016/j.jsb.2014.08.007

519 Fitzer, S.C., Phoenix, V.R., Cusack, M., Kamenos, N.A., 2014b. Ocean acidification impacts
520 mussel control on biomineralisation. Sci. Rep. 4. https://doi.org/10.1038/srep06218

521 Fitzer, S.C., Torres Gabarda, S., Daly, L., Hughes, B., Dove, M., O'Connor, W., Potts, J.,
522 Scanes, P., Byrne, M., 2018. Coastal acidification impacts on shell mineral structure of
523 bivalve mollusks. Ecol. Evol. https://doi.org/10.1002/ece3.4416

524 Fitzer, S.C., Vittert, L., Bowman, A., Kamenos, N.A., Phoenix, V.R., Cusack, M., 2015.
525 Ocean acidification and temperature increase impact mussel shell shape and thickness:
526 Problematic for protection? Ecol. Evol. 5, 4875–4884. https://doi.org/10.1002/ece3.1756

527 Gao, P., Liao, Z., Wang, X.-X., Bao, L.-F., Fan, M.-H., Li, X.-M., Wu, C.-W., Xia, S.-W.,
528 2015. Layer-by-Layer Proteomic Analysis of Mytilus galloprovincialis Shell. PLoS One
529 10, e0133913. https://doi.org/10.1371/journal.pone.0133913

530 Gräwe, U., Friedland, R., Burchard, H., 2013. The future of the western Baltic Sea: Two pos-
531 sible scenarios. Ocean Dyn. https://doi.org/10.1007/s10236-013-0634-0

532 Gustafsson, B.G., Westman, P., 2002. On the causes for salinity variations in the Baltic Sea
533 during the last 8500 years. Paleoceanography 17, 12-1-12–14.
534 https://doi.org/10.1029/2000PA000572

535 Harper EM, Clark MS, Hoffman JI, Philipp EER, Peck LS, et al., 2012. Iceberg Scour and
536 Shell Damage in the Antarctic Bivalve Laternula elliptica. PLOS ONE 7(9): e46341.

https://doi.org/10.1371/journal.pone.0046341 Hayashi, C.Y., Shipley, N.H., Lewis, R. V., 1999. Hypotheses that correlate the sequence, structure, and mechanical properties of spider silk proteins, in: International Journal of Biological Macromolecules. pp. 271–275. https://doi.org/10.1016/S0141-8130(98)00089-0

Hu, X., Cebe, P., Weiss, A.S., Omenetto, F., Kaplan, D.L., 2012. Protein-based composite materials. Mater. Today. https://doi.org/10.1016/S1369-7021(12)70091-3

Hüning, A.K., Melzner, F., Thomsen, J., Gutowska, M.A., Krämer, L., Frickenhaus, S., Rosenstiel, P., Pörtner, H.O., Philipp, E.E.R., Lucassen, M., 2013. Impacts of seawater acidification on mantle gene expression patterns of the Baltic Sea blue mussel: Implications for shell formation and energy metabolism. Mar. Biol. 160, 1845–1861. https://doi.org/10.1007/s00227-012-1930-9

Jackson D.J., McDougall C., Woodcroft B., Moase P., Rose R.A., Kube M., Reinhardt R., Rokhsar D.S., Montagnani C., Joubert C., Piquemal D., Degnan B.M., 2010. Parallel evolution of nacre building gene sets in molluscs. Mol Biol Evol.;27(3):591-608. doi:10.1093/molbev/msp278

Jiravanichpaisal, P., Lee, B.L., Söderhäll, K., 2006. Cell-mediated immunity in arthropods: Hematopoiesis, coagulation, melanization and opsonization. Immunobiology. https://doi.org/10.1016/j.imbio.2005.10.015

Johannesson K., André C., 2006. Life on the margin: genetic isolation and diversity loss in a peripheral marine ecosystem, the Baltic Sea. Mol Ecol.;15(8):2013-2029. doi:10.1111/j.1365-294X.2006.02919.x

Jung, H., Pena-Francesch, A., Saadat, A., Sebastian, A., Kim, D.H., Hamilton, R.F., Albert, I., Allen, B.D., Demirel, M.C., 2016. Molecular tandem repeat strategy for elucidating mechanical properties of high-strength proteins. Proc. Natl. Acad. Sci. 113, 6478–6483.

https://doi.org/10.1073/pnas.1521645113

Kautsky, N., 1982. Growth and size structure in a baltic Mytilus edulis population. Mar. Biol. 68, 117–133. https://doi.org/10.1007/BF00397599

Kautsky, N., Johannesson, K., Tedengren, M., 1990. Genotypic and phenotypic differences between Baltic and North Sea populations of Mytilus edulis evaluated through reciprocal transplantations. I Gorwth and morphology. Mar. Ecol. Prog. Ser. 59, 203–210. https://doi.org/10.3354/meps059203

Knöbel L., Breusing C., Bayer T., Sharma V., Hiller M., Melzner F., Stuckas H., 2020. Comparative de novo assembly and annotation of mantle tissue transcriptomes from the Mytilus edulis species complex (M. edulis, M. galloprovincialis, M. trossulus). Marine Genomics (51), 1874-7787. https://doi.org/10.1016/j.margen.2019.100700

Larsson, J., Lind, E.E., Corell, H. Grahn,, M., Smolarz, K., Lönn, M. 2017. Regional genetic differentiation in the blue mussel from the Baltic Sea area. Estuarine, Coastal and Shelf Science, 195, 98-109, https://doi.org/10.1016/j.ecss.2016.06.016.

Li, H., Wang, D., Deng, Z., Huang, G., Fan, S., Zhou, D., Liu, B., Zhang, B., Yu, D., 2017. Molecular characterization and expression analysis of chitinase from the pearl oyster Pinctada fucata. Comp. Biochem. Physiol. Part B Biochem. Mol. Biol. 203, 141–148. https://doi.org/10.1016/j.cbpb.2016.10.007

Loftus, E., Rogers, K., Lee-Thorp, J., 2015. A simple method to establish calcite: Aragonite ratios in archaeological mollusc shells. J. Quat. Sci. 30, 731–735. https://doi.org/10.1002/jqs.2819

Lowenstam, H.A., 1981. Minerals formed by organisms. Science 211, 1126–1131. https://doi.org/10.1126/science.7008198

584 Luna-Acosta, A., Thomas-Guyon, H., Amari, M., Rosenfeld, E., Bustamante, P., Fruitier-
585 Arnaudin, I., 2011. Differential tissue distribution and specificity of phenoloxidases from
586 the Pacific oyster Crassostrea gigas. Comp. Biochem. Physiol. Part B Biochem. Mol. Bi-
587 ol. 159, 220–226. https://doi.org/10.1016/j.cbpb.2011.04.009

588 Marin F, Luquet G, Marie B, Medakovic D, 2008. Molluscan shell proteins: primary struc-
589 ture, origin, and evolution. Curr Top Dev Biol.;80:209-276. doi:10.1016/S0070-
590 2153(07)80006-8

591 Mackenzie C.L., Ormondroyd G.A,. Curling S.F., Ball R.J., Whiteley N.M., Malham S.K.,
592 2014. Ocean warming, more than acidification, reduces shell strength in a commercial
593 shellfish species during food limitation. PLoS One.;9(1):e86764. Published 2014 Jan 28.
594 doi:10.1371/journal.pone.0086764

595 McDougall C., Degnan B.M., 2018. The evolution of mollusc shells. Wiley Interdiscip Rev
596 Dev Biol.;7(3):e313. doi:10.1002/wdev.313

597 Miyamoto, H., Miyashita, T., Okushima, M., Nakano, S., Morita, T., Matsushiro, A., 1996. A
598 carbonic anhydrase from the nacreous layer in oyster pearls. Proc Natl Acad Sci 93.
599 https://doi.org/10.1073/pnas.93.18.9657

600 Moret, Y., 2003. Explaining variable costs of the immune response: Selection for specific
601 versus non-specific immunity and facultative life history change. Oikos.
602 https://doi.org/10.1034/j.1600-0706.2003.12496.x

603 Morse, J.W., Rolf S. Arvidson, A., Lüttge, A., 2007. Calcium Carbonate Formation and
604 Dissolution. https://doi.org/10.1021/CR050358J

605 Müller, J.D., Schneider, B. and Rehder, G, 2016. Long-term alkalinity trends in the Baltic Sea
606 and their implications for CO2-induced acidification. Limnol. Oceanogr., 61: 1984-2002.

607 doi:10.1002/lno.10349

608 Nakahara, H., Kakei, M., Bevelander, G., 1980. Fine structure and amino acid composition of
609 the organic envelope in the prismatic layer of some bivalve shells. Venus 39, 167–177.

610 Norling, P., Kautsky, N., 2008. Patches of the mussel Mytilus sp. Are islands of high biodi-
611 versity in subtidal sediment habitats in the Baltic Sea. Aquatic Biology. 4.
612 10.3354/ab00096.

613 Ojaveer H., Jaanus A., Mackenzie B.R., Martin G., Olenin S., Radziejewska T., Telesh I. Zet-
614 tler M.L., Zaiko A.., 2010. Status of biodiversity in the Baltic Sea,. PLoS
615 One.;5(9):e12467. Published 2010 Sep 1. doi:10.1371/journal.pone.0012467

616 Perovic I., Chang E.P., Lui M., Rao A., Cölfen H., Evans J.S., 2014. A nacre protein, n16.3,
617 self-assembles to form protein oligomers that dimensionally limit and organize mineral
618 deposits. Biochemistry.;53(16):2739-2748. doi:10.1021/bi401721z

619 Qin, C. li, Pan, Q. dong, Qi, Q., Fan, M. hua, Sun, J. jing, Li, N. nan, Liao, Z., 2016. In-depth
620 proteomic analysis of the byssus from marine mussel Mytilus coruscus. J. Proteomics
621 144, 87–98. https://doi.org/10.1016/j.jprot.2016.06.014

622 Rae, R., 2017. The gastropod shell has been co-opted to kill parasitic nematodes. Sci. Rep. 7.
623 https://doi.org/10.1038/s41598-017-04695-5

624 Reimer, O., Harms-Ringdahl, S., 2001. Predator-inducible changes in blue mussels from the
625 predator-free Baltic Sea. Mar. Biol. 139, 959–965.
626 https://doi.org/10.1007/s002270100606

627 Sanders, T., Schmittmann, L., Nascimento-Schulze, J. C., & Melzner, F., 2018. High Calcifi-
628 cation Costs Limit Mussel Growth at Low Salinity. Frontiers in Marine Science,
629 5(October), 1–9. https://doi.org/10.3389/fmars.2018.00352.

630 Stuckas, H., Knöbel, L., Schade, H., Breusing, C., Hinrichsen, H.-H., Bartel, M., Langguth,
631 K. and Melzner, F., 2017. Combining hydrodynamic modelling with genetics: can pas-
632 sive larval drift shape the genetic structure of Baltic Mytilus populations?. Mol Ecol, 26:
633 2765-2782. https://doi:10.1111/mec.14075

634 Suzuki, M., Iwashima, A., Tsutsui, N., Ohira, T., Kogure, T., Nagasawa, H., 2011. Identifica-
635 tion and characterisation of a calcium carbonate-binding protein, blue mussel shell pro-
636 tein (BMSP), from the nacreous layer. ChemBioChem 12, 2478–2487.
637 https://doi.org/10.1002/cbic.201100317

638 Telesca, L., Peck, L.S., Sanders, T., Thyrring, J., Sejr, M.K., Harper, E.M., 2019. Biomineral-
639 ization plasticity and environmental heterogeneity predict geographical resilience pat-
640 terns of foundation species to future change. Glob. Chang. Biol.
641 https://doi.org/10.1111/gcb.14758

642 Thomsen, J., Gutowska, M.A., Saphörster, J., Heinemann, A., Trübenbach, K., Fietzke, J.,
643 Hiebenthal, C., Eisenhauer, A., Körtzinger, A., Wahl, M., Melzner, F., 2010. Calcifying
644 invertebrates succeed in a naturally CO2-rich coastal habitat but are threatened by high
645 levels of future acidification. Biogeosciences 7, 3879–3891. https://doi.org/10.5194/bg-
646 7-3879-2010

647 Thomsen, J., Stapp, L.S., Haynert, K., Schade, H., Danelli, M., Lannig, G., Wegner, K.M.,
648 Melzner, F., 2017. Naturally acidified habitat selects for ocean acidification–tolerant
649 mussels. Sci. Adv. 3. https://doi.org/10.1126/sciadv.1602411

650 Tyrrell, T., Schneider, B., Charalampopoulou, a., & Riebesell, U. 2008. Coccolithophores and
651 calcite saturation state in the Baltic and Black Seas. Biogeosciences, 5, 485–494.
652 https://doi.org/10.5194/bgd-4-3581-2007

653 Väinölä and Strelkov, P., 2011. Mytilus trossulus in northern Europe. Mar. Biol. 158,

817e833

Vuorinen, I., & Antsulevich, Alexander E, M. N. V., 2002. Spatial distribution and growth of the common mussel Mytilus edulis L . in the archipelago of. Boreal Environment Research, 7, 41–52

Waldbusser, G.G., Hales, B., Langdon, C.J., Haley, B.A., Schrader, P., Brunner, E.L., Gray, M.W., Miller, C.A., Gimenez, I., 2015. Saturation-state sensitivity of marine bivalve larvae to ocean acidification. https://doi.org/10.1038/NCLIMATE2479

Weiner, S., 1979. Aspartic acid-rich proteins: major components of the soluble organic matrix of mollusk shells. Calcif. Tissue Int. 29, 163–7. https://doi.org/10.1007/BF02408072

Weiner, S., Traub, W., 1980. X-ray diffraction study of the insoluble organic matrix of mollusk shells. FEBS Lett. 111, 311–316. https://doi.org/10.1016/0014-5793(80)80817-9

Wu, F., Falfushynska, H., Dellwig, O., Piontkivska, H., Sokolova, I.M., 2020. Interactive effects of salinity variation and exposure to ZnO nanoparticles on the innate immune system of a sentinel marine bivalve, Mytilus edulis. Sci. Total Environ. https://doi.org/10.1016/j.scitotenv.2019.136473

Yonezawa, M., Sakuda, S., Yoshimura, E., Suzuki, M., 2016. Molecular cloning and functional analysis of chitinases in the fresh water snail, Lymnaea stagnalis. J. Struct. Biol. https://doi.org/10.1016/j.jsb.2016.02.021

Zhang, C., Xie, L., Huang, J., Chen, L., Zhang, R., 2006. A novel putative tyrosinase involved in periostracum formation from the pearl oyster (Pinctada fucata). Biochem. Biophys. Res. Commun. 342, 632–639. https://doi.org/10.1016/j.bbrc.2006.01.182

Data availability

The mass spectrometry proteomics data have been deposited to the ProteomeXchange Consortium *via* the PRIDE partner repository with the dataset identifiers PXD013091 and 10.6019/PXD013091; PXD013148 and 10.6019/PXD013148.

Acknowledgements

This study was supported by the funding from the CACHE (CAlcium in a CHanging Environment) initial training network (ITN) of the European Union Seventh Framework Program. Reference grant agreement number 605051. We thank F. Melzner and T. Sanders for sharing the shell samples collected under the CACHE program and for their helpful discussions and suggestions in preparing the manuscript. We acknowledge H. Stuckas for sharing the transcriptome databases. We thank E. Dufour for shell sample preparation facility and G. Toutirais for microscopy experiments.

†Present address: Proteomics Center of Excellence, Northwestern University, Chicago, IL-60611, USA

*To whom correspondence may be addressed. Email: arul.marie@mnhn.fr

Author contributions: A.M. and S.B. designed the experiments; J.A. prepared the samples for proteomic experiments; G.C. and J.V. performed mass spectrometry analysis; J.A., B.M. and A.M. analyzed the mass spectrometry data and validated the results; J.A. and S.B. generated scanning electron microscopy images. S.M.Z. carried out the compression tests. P.D. is a Research Director of the National Fund for Scientific Research (Belgium), designed the compression tests and analyzed the results. M.L. ran FTIR analysis and S.B. performed statistical analysis. J.A., S.B. and A.M. wrote the paper and all authors discussed and approved the manuscript.

The authors declare no conflict of interest

Legends for Figures and Tables:

Figure 1:

(a) Mussel sampling locations. (b) Dot plot indicates the size range of the blue mussel shells are homogenous and the histogram shows the shell fracture reistance (F_{max}) of shells from different sites. F_{max} of shells from North Sea (Sylt) varies considerably compared to shells from Baltic Sea (Nynäshamn and Usedom; Kruskal-wallis chi-squared =8.43, *p-value* = 0.01). (c) FT-IR of aragonite and calcite reference materials. (d) FT-IR spectra of North Sea (Sylt) and mussel shell samples show highly superimposable spectra. Panels (e) and (f) represents scatter and box plot of IR peak absorbance ratio 875/1785 (kruskal-wallis chi-squared = 0.78, *p-value* = 0.67) and 1793/1785 (kruskal-wallis chi-squared = 0.86, *p-value* = 0.65) respectively indicating that shells from Sylt, Usedom and Nynäshman consist of rather similar mixture of aragonite and calcite. Red line in the panel e represents 100% calcite

Figure 2:

Scanning electron microscopy images show altered microstructure of Baltic mytilid shells. The region of the shell used for acquiring the images is shown at the top. Rows a, b and c show the interface of the nacreous layer, myostracum and prismatic layer of the shells from Sylt, Usedom and Nynäshman respectively. Each row followed by magnified images of nacreous and prismatic layers. In Baltic mytilid mussels (rows b and c) the nacreous layer is formed by relatively thin aragonite tablets compared to North Sea mussels (row a). Ladders in the nacre layer are shown for visualizing tablet thickness. Prismatic layers are formed by irregular calcite prisms in Baltic mytilid mussels and are indicated by arrows

Figure 3:

Gene ontology (GO) count of molecular functions represented using the matched transcripts from *M. edulis* and *M.trossulus* databases

Figure 4:

Heat map generated using Label free LC-MS/MS data indicating modulated SMPs identified with *M. trossulus* transcriptome database

Figure 5:

Simulated structure of proteins TR78416 and TR71052 predicted using the I-Tasser tool (a and b respectively). TR78416 proteins contain motifs that are formed by β-strand-turn-β-strand and are similar

to that of spider silk. (c) β-roll structure formed by GAGAGAGX repeats of *B. Mori* silk protein. Primary protein sequences are given for both the proteins and the GGXGG repeating motifs (see text) are shaded in yellow.

Figure 6:

The phenoloxidase (PO) pathway in arthropods and crustaceans indicating the different proteins that are modulated in Baltic mussels under the influence of low salinity and biotic factors that characterize their habitat. Down-regulated proteins are represented in green font and up- regulated proteins are denoted in red font.

Supplementary Figure 1:

(a) Graph shows periostracum/mineral layer thickness ratio (expressed as %) of shells from three locations and clusters into separate groups Baltic mussels (Nynäshman and Usedom) and North Sea mussels (Sylt). Boxplots constructed with periostracum thickness/mineral layer thickness ratio (as %) and mineral layer thickness illustrates the separation of the Baltic and North Sea shells. (b) Box plot showing the organic content of the shells excluding periostracum. (c) Principal component analysis performed by combining mineral layer thickness (Mn), periostracum thickness (P) and organic content (OC) separates the Baltic mussels from the North Sea mussels.

Supplementary figure 2:

Heat map generated using Label free LC-MS/MS data showing modulated SMPs that are identified using *M.edulis* transcriptome database.

Supplementary Table 1:

List of matched transcripts from *M.trossulus* and *M.edulis* database using Mascot and grouped using Scaffold software. The list indicates proteins and proteoforms from all the three sites matched to each database.

Supplementary Table 2:

List of matched proteins from Supplementary Table 1 and annotated using BLAST.

Supplementary Table 3:

Combined list of modulated SMPs and corresponding SMART functional domains from *M. trossulus* (Figure 4) and the *M. edulis* (Supplementary Figure 2) databases.

760


a
Baltic sea
Nsh
Sylt
Usd
0
500
1000 Km

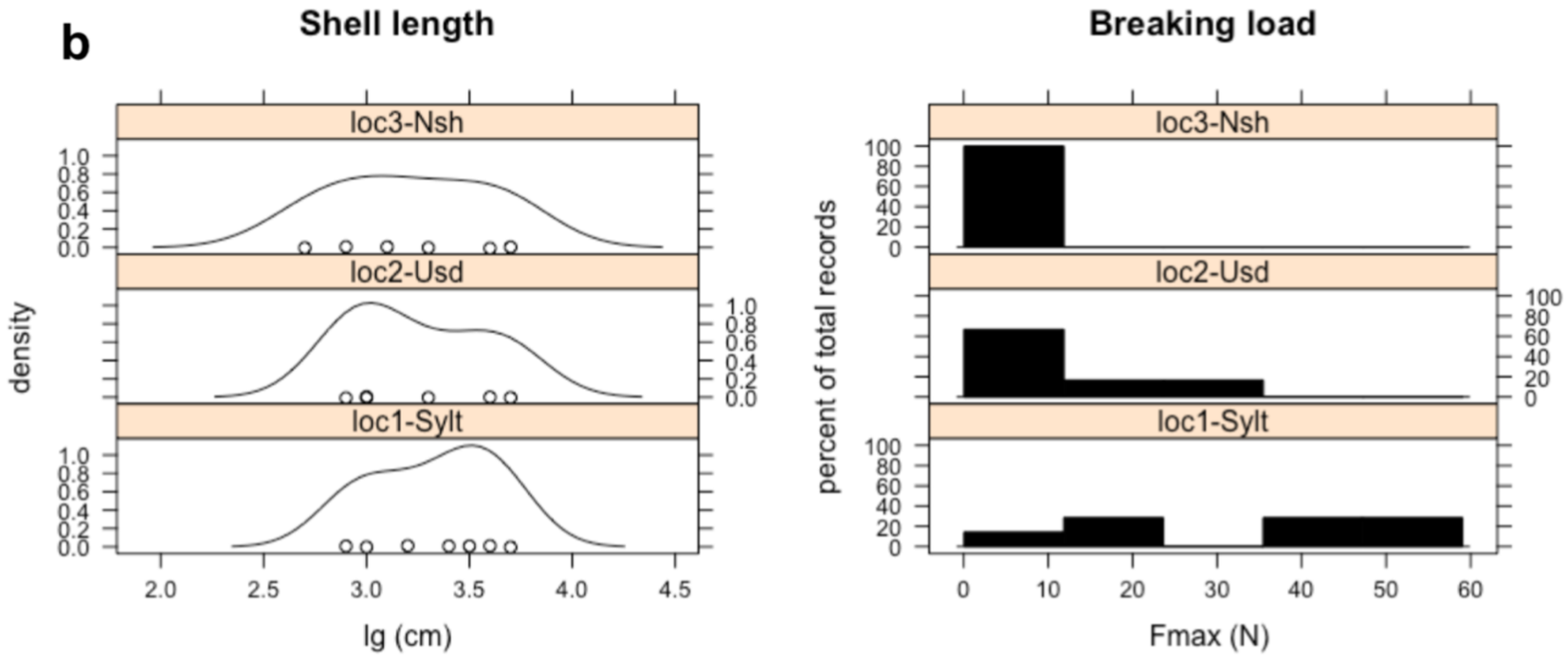
b
Shell length
loc3-Nsh
loc2-Usd
loc1-Sylt
density
lg (cm)
Breaking load
percent of total records
Fmax (N)

FTIR - ATR

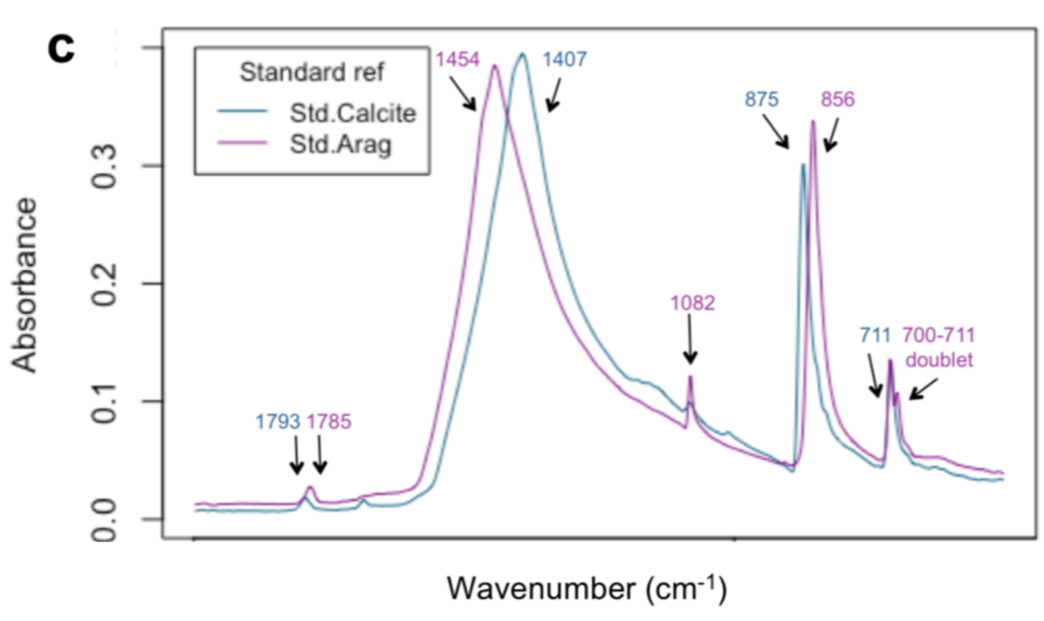
c
Standard ref
Std.Calcite
Std.Arag
1454
1407
875
856
1082
711
700-711
doublet
1793 1785
Absorbance
Wavenumber (cm-1)

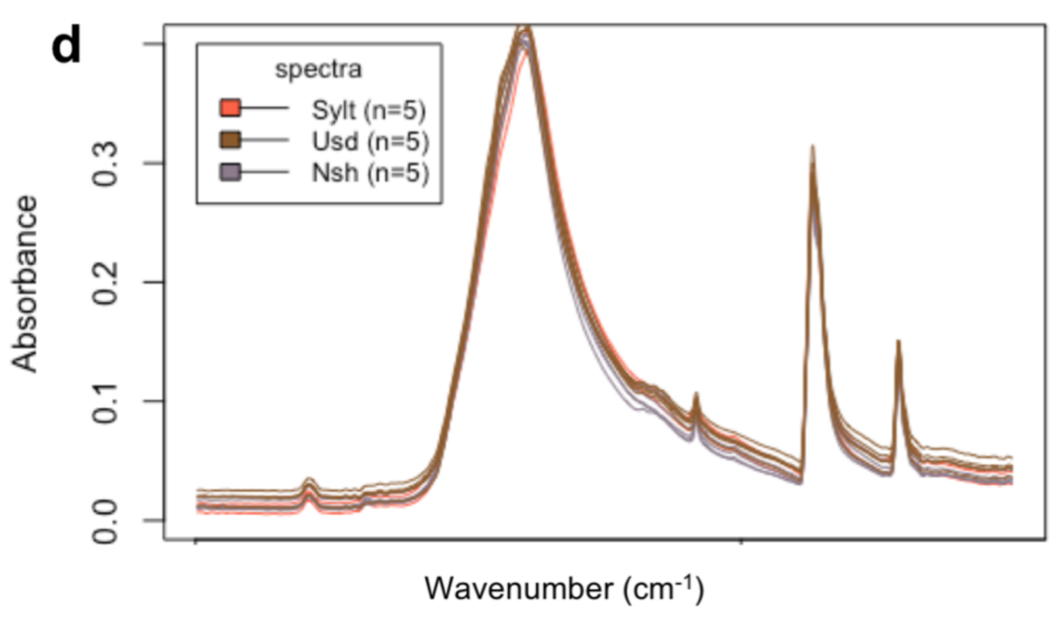
d
spectra
Sylt (n=5)
Usd (n=5)
Nsh (n=5)
Absorbance
Wavenumber (cm-1)

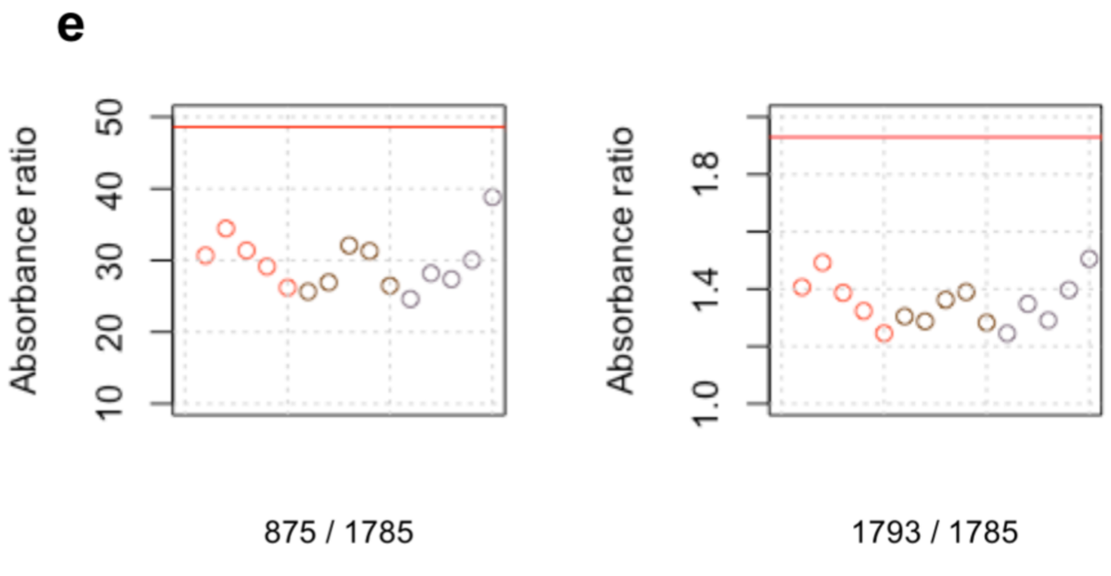
e
Absorbance ratio
875 / 1785
Absorbance ratio
1793 / 1785

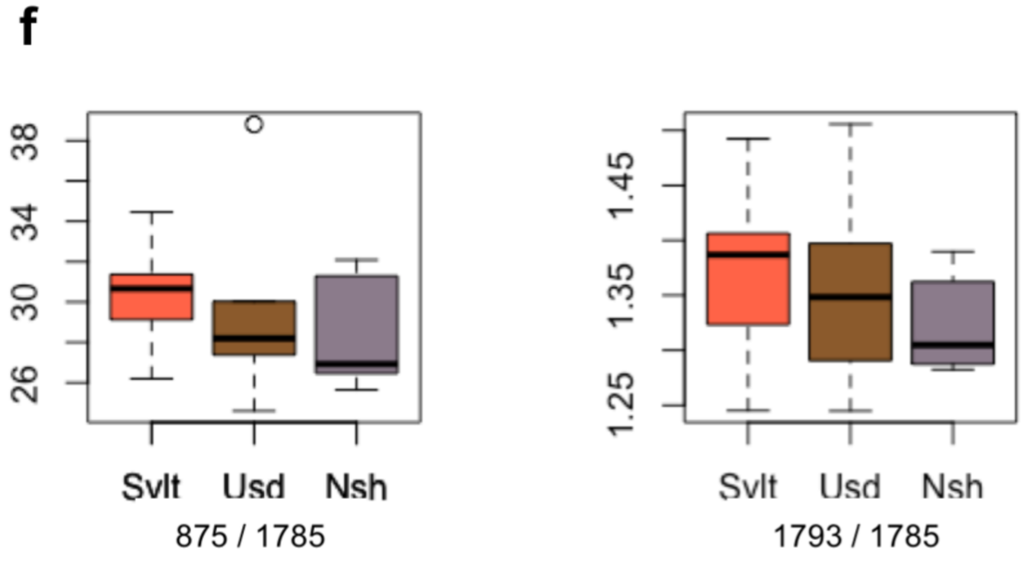
f
Sylt
Usd
Nsh
875 / 1785
Sylt
Usd
Nsh
1793 / 1785

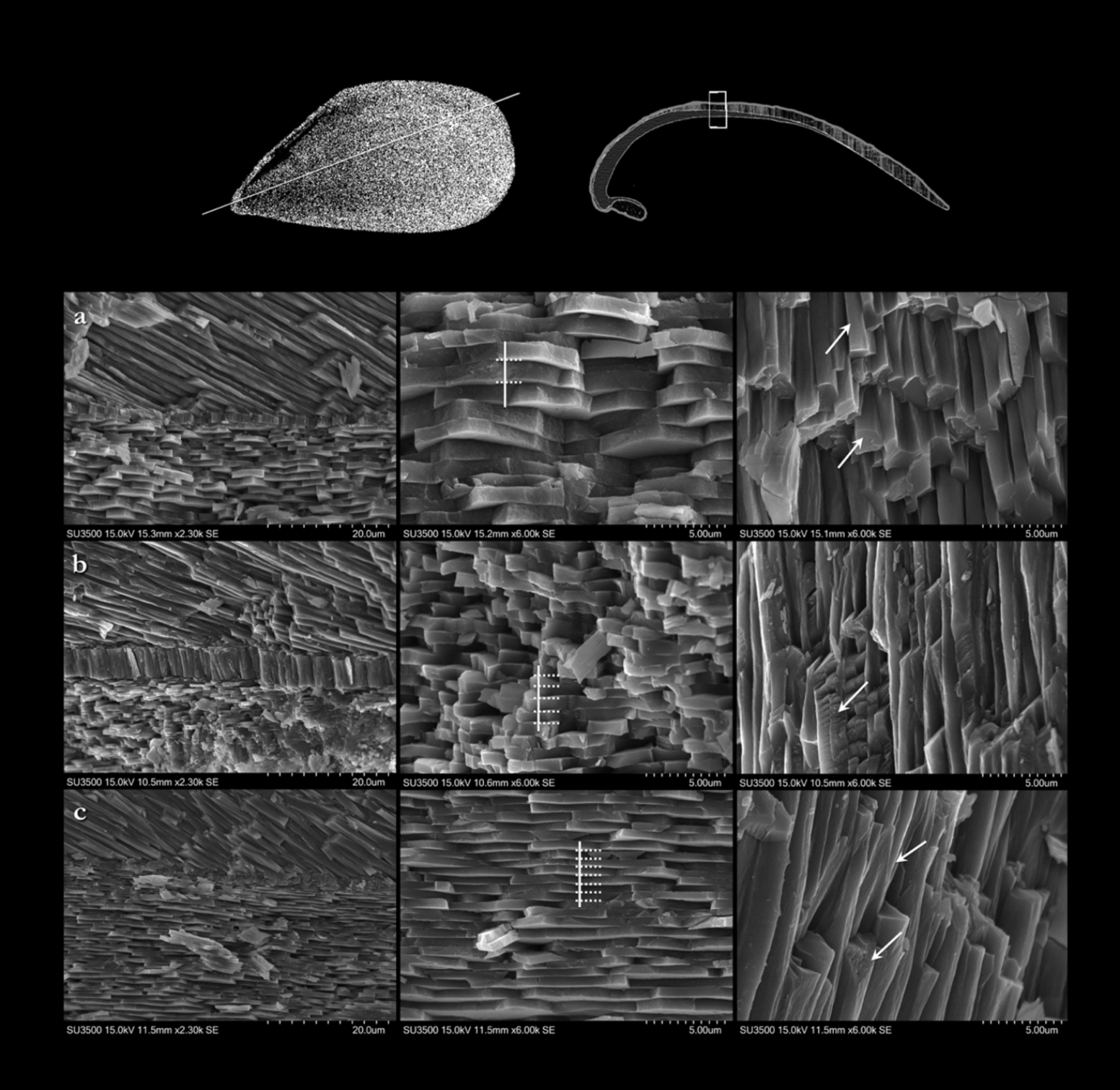
a
SU3500 15.0kV 15.3mm x2.30k SE
20.0um
SU3500 15.0kV 15.2mm x6.00k SE
5.00um
SU3500 15.0kV 15.1mm x6.00k SE
5.00um
b
SU3500 15.0kV 10.5mm x2.30k SE
20.0um
SU3500 15.0kV 10.6mm x6.00k SE
5.00um
SU3500 15.0kV 10.5mm x6.00k SE
5.00um
c
SU3500 15.0kV 11.5mm x2.30k SE
20.0um
SU3500 15.0kV 11.5mm x6.00k SE
5.00um
SU3500 15.0kV 11.5mm x6.00k SE
5.00um

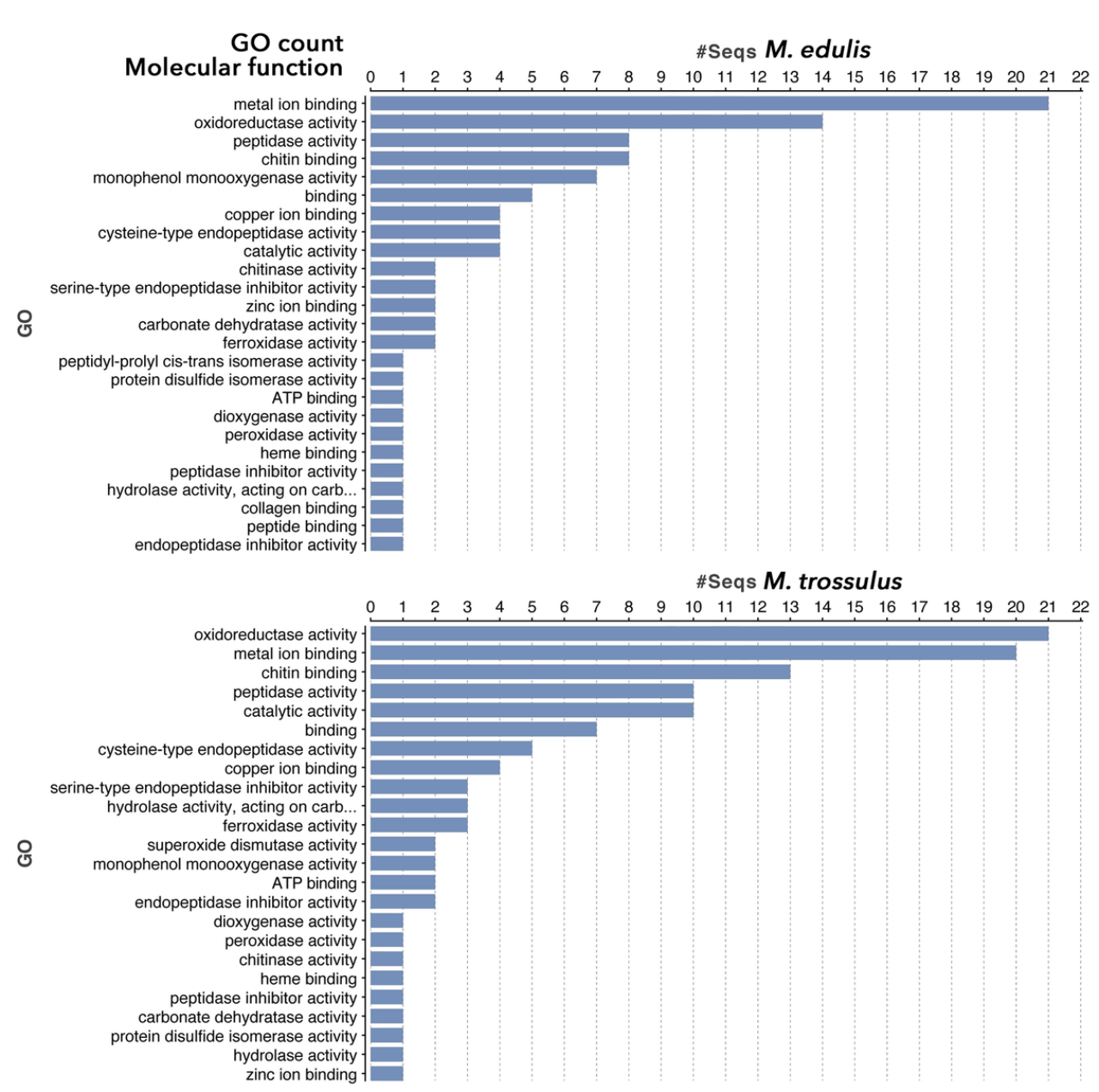
GO count
Molecular function
#Seqs M. edulis
0 1 2 3 4 5 6 7 8 9 10 11 12 13 14 15 16 17 18 19 20 21 22
GO
metal ion binding
oxidoreductase activity
peptidase activity
chitin binding
monophenol monooxygenase activity
binding
copper ion binding
cysteine-type endopeptidase activity
catalytic activity
chitinase activity
serine-type endopeptidase inhibitor activity
zinc ion binding
carbonate dehydratase activity
ferroxidase activity
peptidyl-prolyl cis-trans isomerase activity
protein disulfide isomerase activity
ATP binding
dioxygenase activity
peroxidase activity
heme binding
peptidase inhibitor activity
hydrolase activity, acting on carb...
collagen binding
peptide binding
endopeptidase inhibitor activity
#Seqs M. trossulus
0 1 2 3 4 5 6 7 8 9 10 11 12 13 14 15 16 17 18 19 20 21 22
GO
oxidoreductase activity
metal ion binding
chitin binding
peptidase activity
catalytic activity
binding
cysteine-type endopeptidase activity
copper ion binding
serine-type endopeptidase inhibitor activity
hydrolase activity, acting on carb...
ferroxidase activity
superoxide dismutase activity
monophenol monooxygenase activity
ATP binding
endopeptidase inhibitor activity
dioxygenase activity
peroxidase activity
chitinase activity
heme binding
peptidase inhibitor activity
carbonate dehydratase activity
protein disulfide isomerase activity
hydrolase activity
zinc ion binding

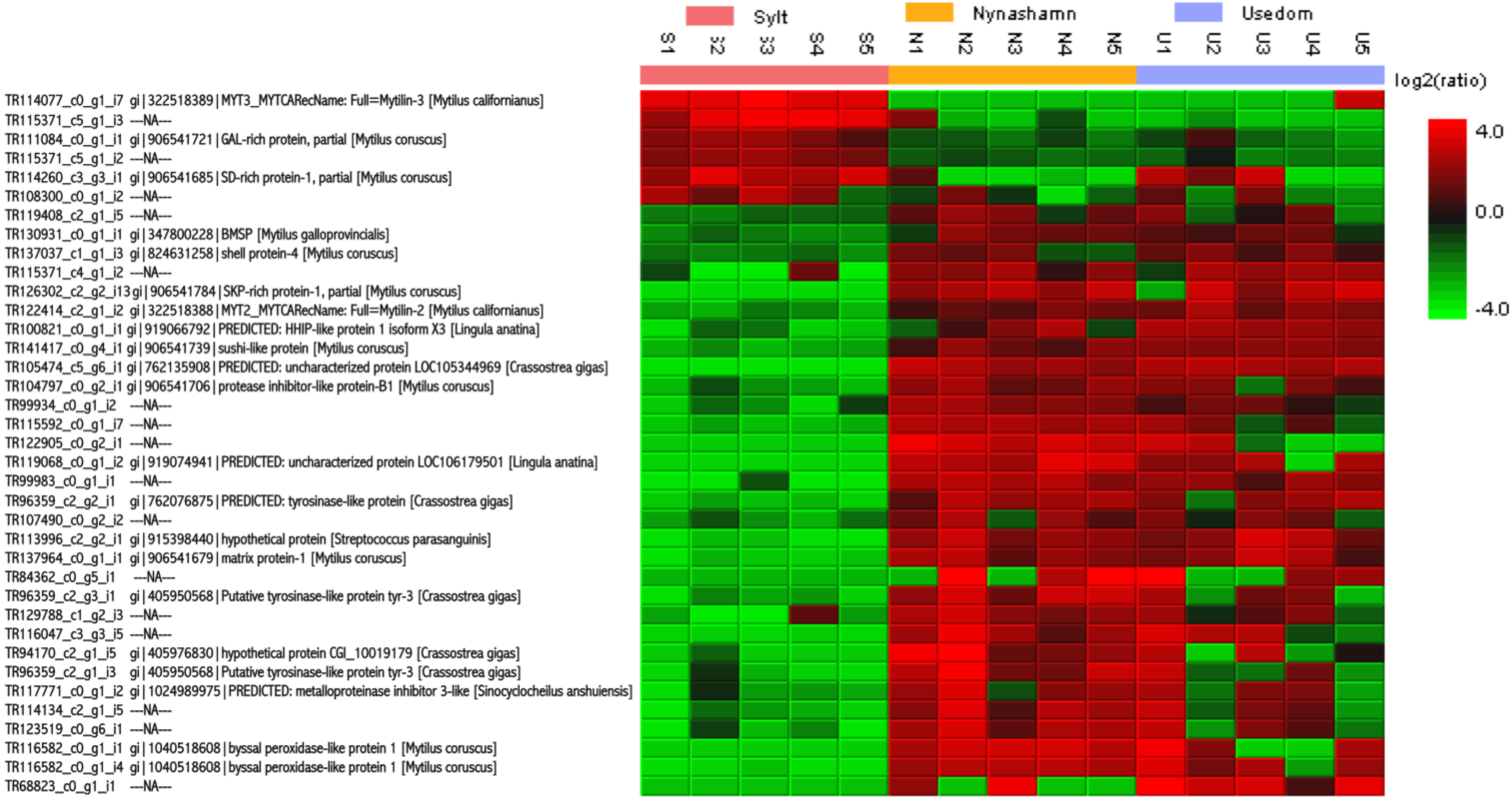
Sylt
Nynashamn
Usedom
S1
S2
S3
S4
S5
N1
N2
N3
N4
N5
U1
U2
U3
U4
U5
log2(ratio)
4.0
0.0
-4.0
TR114077_c0_g1_i7 gi|322518389|MYT3_MYTCARecName: Full=Mytilin-3 [Mytilus californianus]
TR115371_c5_g1_i3 ---NA---
TR111084_c0_g1_i1 gi|906541721|GAL-rich protein, partial [Mytilus coruscus]
TR115371_c5_g1_i2 ---NA---
TR114260_c3_g3_i1 gi|906541685|SD-rich protein-1, partial [Mytilus coruscus]
TR108300_c0_g1_i2 ---NA---
TR119408_c2_g1_i5 ---NA---
TR130931_c0_g1_i1 gi|347800228|BMSP [Mytilus galloprovincialis]
TR137037_c1_g1_i3 gi|824631258|shell protein-4 [Mytilus coruscus]
TR115371_c4_g1_i2 ---NA---
TR126302_c2_g2_i13 gi|906541784|SKP-rich protein-1, partial [Mytilus coruscus]
TR122414_c2_g1_i2 gi|322518388|MYT2_MYTCARecName: Full=Mytilin-2 [Mytilus californianus]
TR100821_c0_g1_i1 gi|919066792|PREDICTED: HHIP-like protein 1 isoform X3 [Lingula anatina]
TR141417_c0_g4_i1 gi|906541739|sushi-like protein [Mytilus coruscus]
TR105474_c5_g6_i1 gi|762135908|PREDICTED: uncharacterized protein LOC105344969 [Crassostrea gigas]
TR104797_c0_g2_i1 gi|906541706|protease inhibitor-like protein-B1 [Mytilus coruscus]
TR99934_c0_g1_i2 ---NA---
TR115592_c0_g1_i7 ---NA---
TR122905_c0_g2_i1 ---NA---
TR119068_c0_g1_i2 gi|919074941|PREDICTED: uncharacterized protein LOC106179501 [Lingula anatina]
TR99983_c0_g1_i1 ---NA---
TR96359_c2_g2_i1 gi|762076875|PREDICTED: tyrosinase-like protein [Crassostrea gigas]
TR107490_c0_g2_i2 ---NA---
TR113996_c2_g2_i1 gi|915398440|hypothetical protein [Streptococcus parasanguinis]
TR137964_c0_g1_i1 gi|906541679|matrix protein-1 [Mytilus coruscus]
TR84362_c0_g5_i1 ---NA---
TR96359_c2_g3_i1 gi|405950568|Putative tyrosinase-like protein tyr-3 [Crassostrea gigas]
TR129788_c1_g2_i3 ---NA---
TR116047_c3_g3_i5 ---NA---
TR94170_c2_g1_i5 gi|405976830|hypothetical protein CGI_10019179 [Crassostrea gigas]
TR96359_c2_g1_i3 gi|405950568|Putative tyrosinase-like protein tyr-3 [Crassostrea gigas]
TR117771_c0_g1_i2 gi|1024989975|PREDICTED: metalloproteinase inhibitor 3-like [Sinocyclocheilus anshuiensis]
TR114134_c2_g1_i5 ---NA---
TR123519_c0_g6_i1 ---NA---
TR116582_c0_g1_i1 gi|1040518608|byssal peroxidase-like protein 1 [Mytilus coruscus]
TR116582_c0_g1_i4 gi|1040518608|byssal peroxidase-like protein 1 [Mytilus coruscus]
TR68823_c0_g1_i1 ---NA---

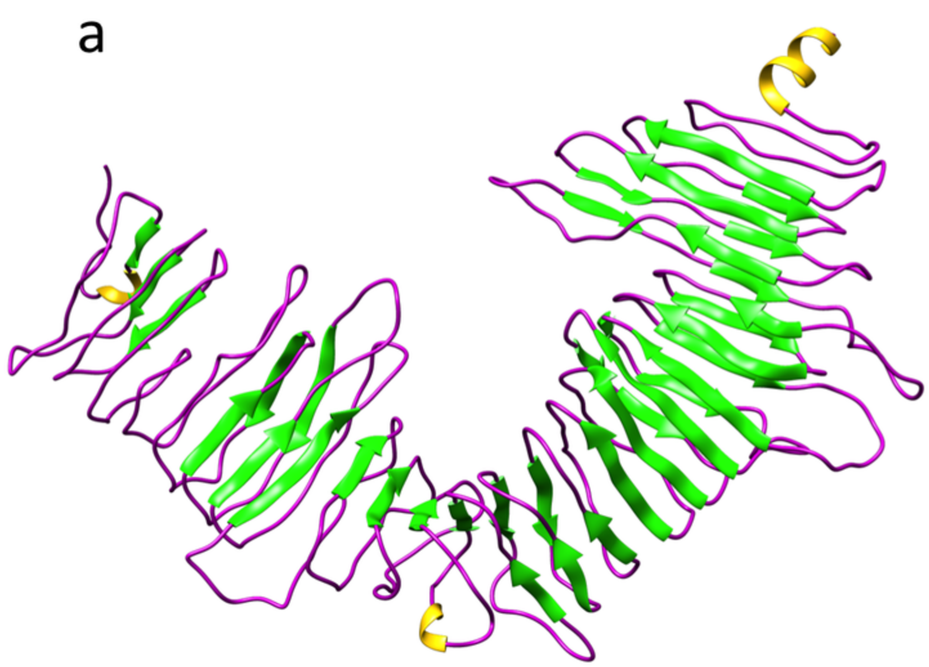

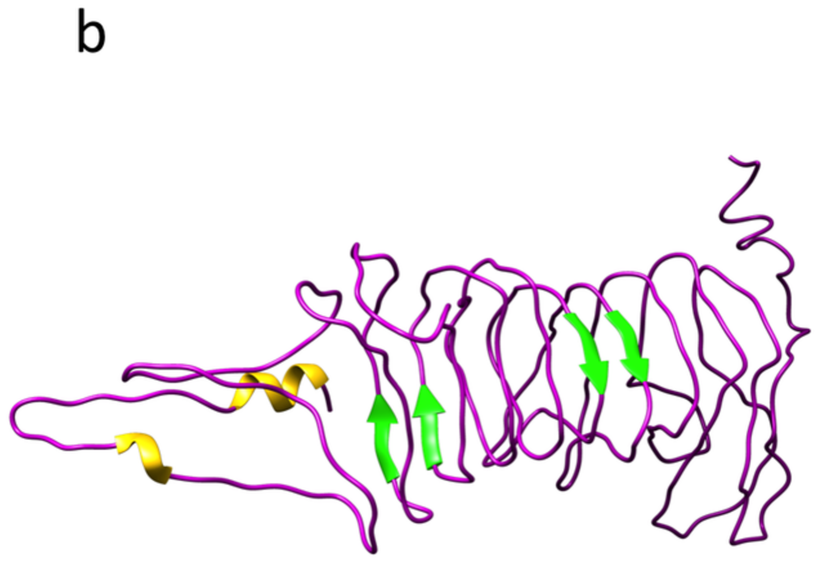

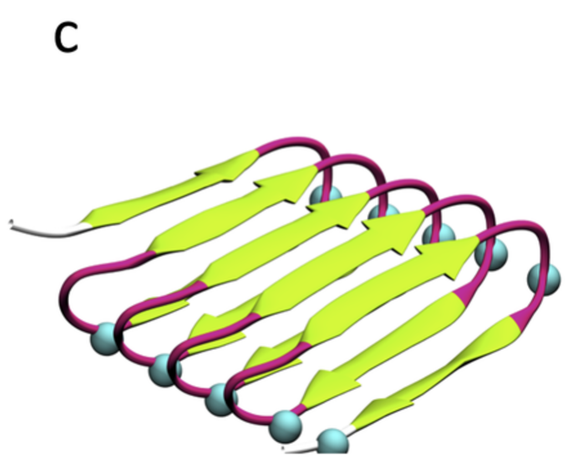

a: TR78416_c0_g1_i2

GAGAGGAGAGGSGAGGAGGSGAGGAGGAGGDGDCESSDSDSGSDSDSDNDTDSSDSDTGSDASDSDSGSDPD
GDGDSDSSGTSESSESSDSDYSSDDDDEESESDDSFRSAAKIIIQLLTRLLMSGGLGGAGSSASASASAGAAAGGAG
GAGLGFGGWGGAGAGASAAAAAAAAAGAGGFGGVGGYGGGASAQAFAAASAAAAAARRAKLLNLLFSRSSAS
AAAIAAASARAGAGGGFGGRFGGRAAAGASASAGASAGGGGNDGGSSSAAAAAAAAAAAAARNANLRGWLVAS
GVGAGAGAGAGAGGFGSGGGGGGGSGGSGGSGGSGGSGSSNNNDGNNDTSNNGVKLYAYDYYKDDNSKSSG
YENSK

b: TR71052_c0_g1_i1

AGAGAGAGAGSGAGGAAAAAAAAAAAASGGGGGAGWWNWLGGSGGSSAAAAAAAAAGAGAGGGRKGGR
GGSSAAAAAAAAASSGGGGGYGGKFLGGYGAGSGAAAAAAAAAAAAAANNGGYGGWNGAGGSAAAAAAAA
AAAAGGGGWGGAGGSAAAAAAAAAAAGGGGWGGNGGSAAAAAAAAAASAGGNDGGAASAAAAAAAAA
MAGADAEAVASAYALALAGGNQGLAWMLTSGNDDLRNAAAVAIASASAGVGGGSGGGGGGSGGGGSGGGGGS
GGGGSGGSGGSGGSGSNGKDCTNNEDDDECKKENYN

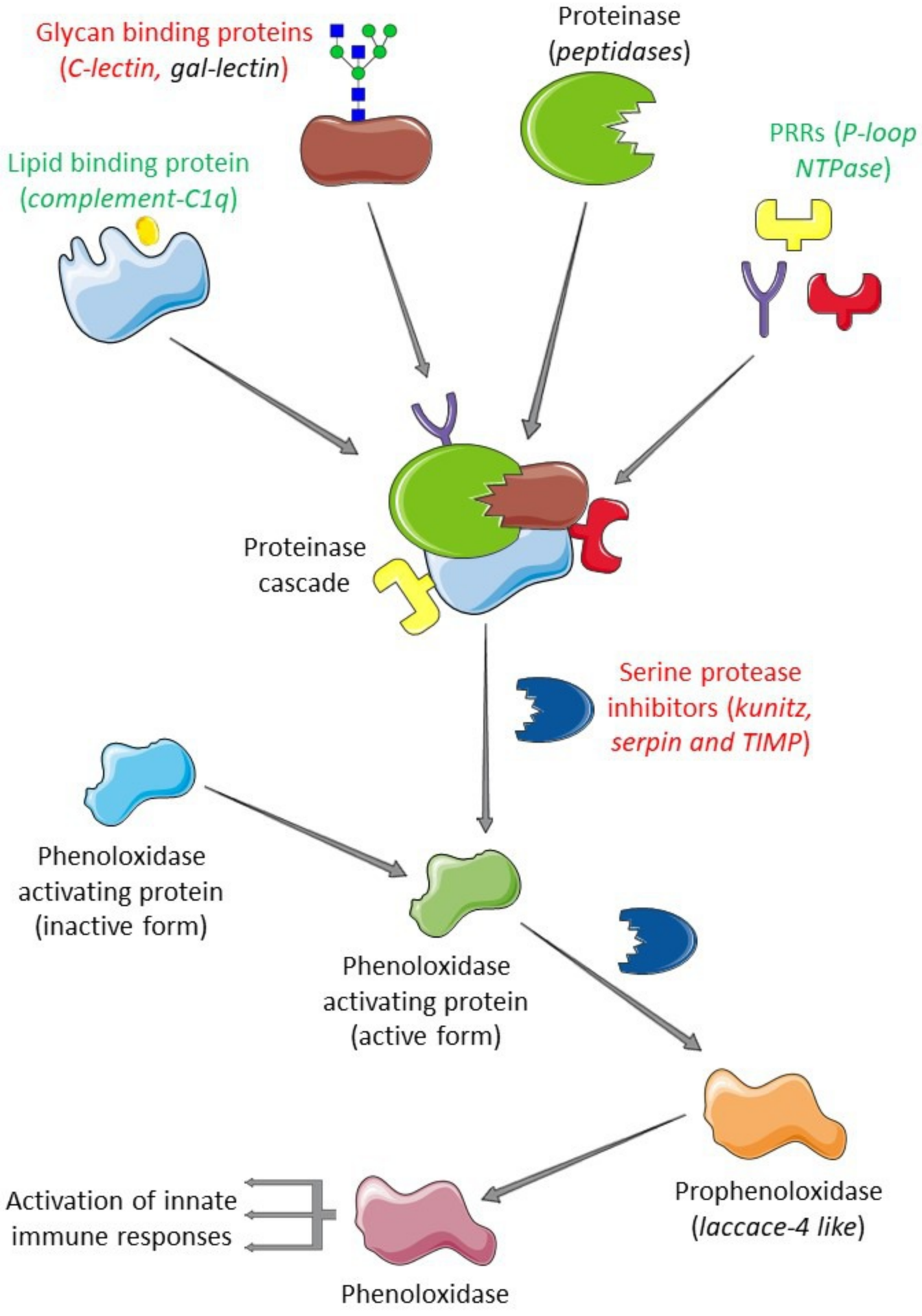
Glycan binding proteins
(C-lectin, gal-lectin)
Proteinase
(peptidases)
Lipid binding protein
(complement-C1q)
PRRs (P-loop
NTPase)
Proteinase
cascade
Serine protease
inhibitors (kunitz,
serpin and TIMP)
Phenoloxidase
activating protein
(inactive form)
Phenoloxidase
activating protein
(active form)
Prophenoloxidase
(laccace-4 like)
Activation of innate
immune responses
Phenoloxidase

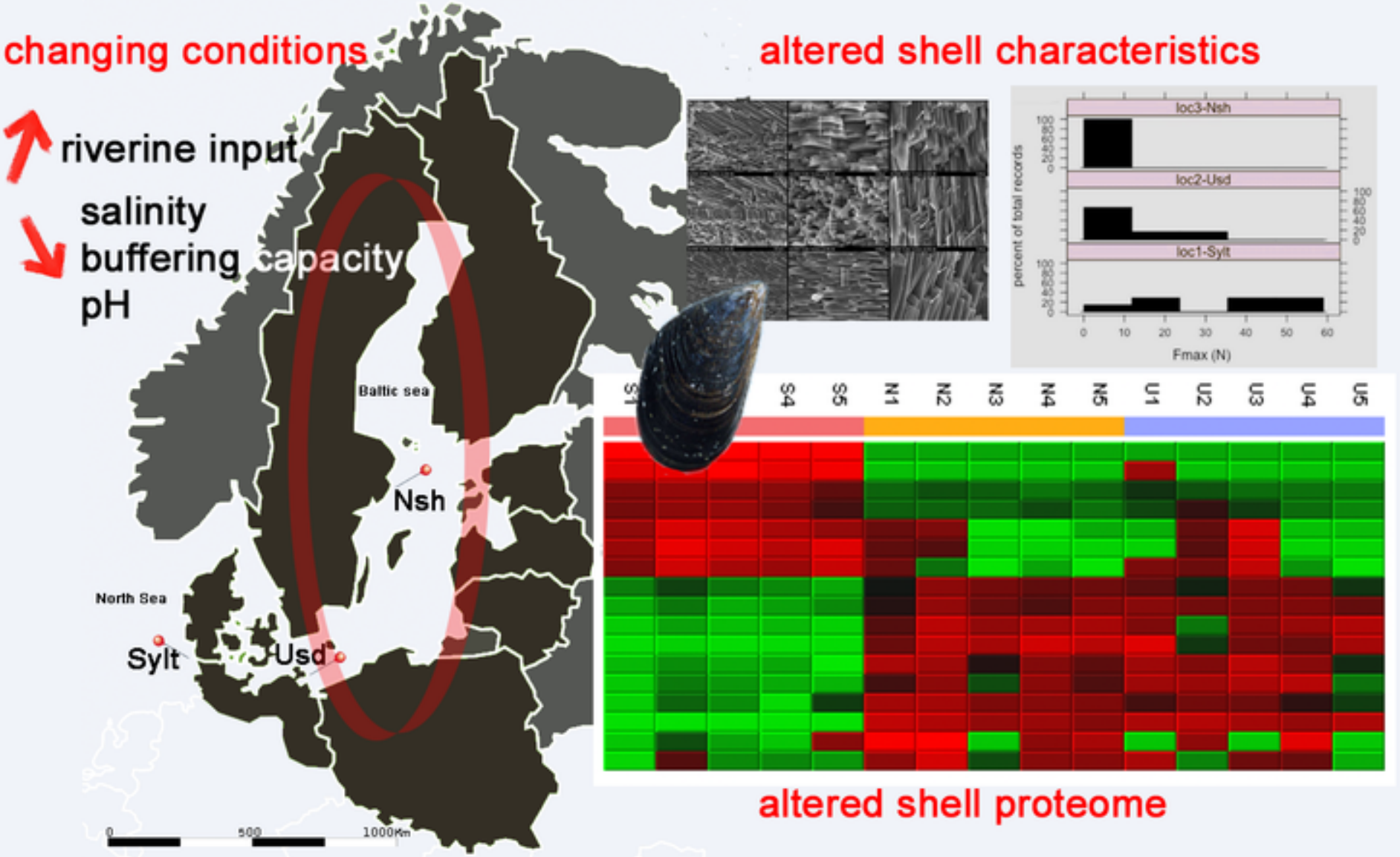
changing conditions
riverine input
salinity
buffering capacity
pH
Baltic sea
Nsh
North Sea
Sylt
Usd
0
500
1000Km
altered shell characteristics
loc3-Nsh
loc2-Usd
loc1-Sylt
percent of total records
Fmax (N)
S1
S4
S5
N1
N2
N3
N4
N5
U1
U2
U3
U4
U5
altered shell proteome